Influence of Ion Bombardment on Electron Emission of MgO Surface in AC Plasma Display Panel

Choon-Sang Park, Heung-Sik Tae, *Senior Member, IEEE*, Eun-Young Jung, Jeong Hyun Seo, and Bhum Jae Shin

Abstract—The influence of ion bombardment during a sustain discharge on the electron emission of the MgO surface and related driving characteristics of an ac plasma display panel were examined using the cathodoluminescence technique and SIMS analysis. The experimental results showed that severe ion bombardment predominantly sputtered Mg species from the MgO surface, thereby lowering the intensity of the F^+ center peak to 3.2 eV due to the elimination of the oxygen vacancy and finally increasing the formative address delay time (T_f) due to an aggravated electron emission capability. Meanwhile, severe ion bombardment also destroyed the shallow trap level, thereby lowering the intensity of the shallow peak to 1.85 eV and eventually increasing the statistical address delay time (T_s) due to a poor electron emission capability from the shallow level. Finally, the aggravated electron emission capability from the shallow level resulted in a reduced wall voltage variation during the address period.

Index Terms—Cathodoluminescence (CL), electron emission, formative address delay time, ion bombardment, statistical address delay time, wall voltage variation.

I. INTRODUCTION

THE SURFACE state of the MgO layer in the front panel is important for producing stable reset and address discharges in plasma display panel (PDP) cells, as the discharge characteristics vary depending on the state of the MgO surface. The MgO layer is used as a protective or electron emission layer in ac PDPs due to its strong resistance to ion sputtering and high secondary electron emission coefficient [1]–[6]. Reducing the statistical address delay (T_s) has recently attracted research attention in order to produce a fast address discharge in plasma displays with very small discharge cells, such as full high definition (FHD) or Quad FHD (QFHD) panels. In this context, the exoelectron emissions of the MgO layer can help to reduce the statistical address delay (T_s) [7], as the exoelectrons emitted from a MgO layer with a shallow trap level act as priming particles to facilitate a fast ignition of the plasma [3]–[5], [7]–[13]. However, the analysis and

measurement of the exoelectron emission emitted from a MgO layer in the PDP cell were very difficult because the defects located at shallow levels with about 0.1–0.5 eV were close to the conduction band. As such, the correlations between the exoelectron emission and the luminescence characteristics were still not fully understood [9], [11], [12].

Consequently, a MgO layer with a shallow trap level is a very important factor for fast and stable PDP driving, particularly in FHD or QFHD PDPs. During the MgO growth process, a small amount of hydrogen gas is allowed to flow in order to form a shallow trap level within the MgO layer [14]. The behavior of a MgO layer with a shallow trap level can be measured using the cathodoluminescence (CL) technique [10]. The CL technique measures the defect levels of a MgO film that can produce visible radiation ranging from 1.8 to 3.5 eV. In this study, the MgO surface characteristics were found to vary depending on the severity of the ion bombardment of the MgO surface with an aging discharge. Moreover, experiments showed that variations in the electron emission of the MgO layer, particularly electron emissions related to the F^+ center peak or electron emissions related to a shallow peak, with respect to the ion bombardment were very important for determining the formative and statistical address delay times $(T_f$ and $T_s)$ and wall charge retention capability, all of which have an influence on creating a stable driving margin for a PDP. In particular, wall voltage behavior that can constantly maintain wall charges from the first to the last scan line is very important for a stable driving margin in a PDP. Nonetheless, these issues have not yet been extensively explored. Thus, the relation between the electron emission characteristics of the MgO layer and the ion bombardment needs to be understood more clearly for the stable driving of a PDP with millions of microdischarge cells.

Accordingly, this study used CL measurements to investigate the changes in the MgO surface characteristics induced by ion bombardment, and examined the resultant changes in the T_f and T_s delay times, including the wall voltage variation (ΔV_w). The number of sustain pulses applied was controlled to produce various sputtered MgO surface states by ion bombardment, and the CL intensity and address discharge characteristics were then investigated in a 42-in panel.

II. EXPERIMENTAL SETUP

Fig. 1 shows the optical measurement systems and commercial 42-in ac-PDP module with three electrodes that were used in the experiment, where X is the sustained electrode, Y is the scan electrode, and A is the address electrode. A pattern generator, a signal generator, and a photosensor amplifier (Hamamatsu C6386) were used to measure the IR emission
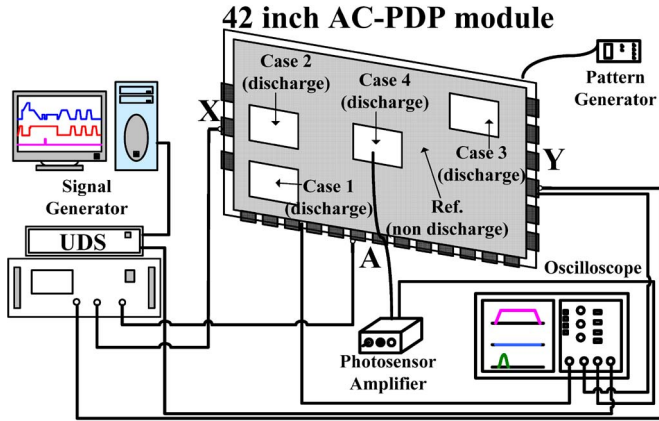
42 inch AC-PDP module

Fig. 1. Schematic diagram of the experimental setup employed in this study.

TABLE I
SPECIFICATIONS OF A 42-IN AC PDP USED IN THIS STUDY

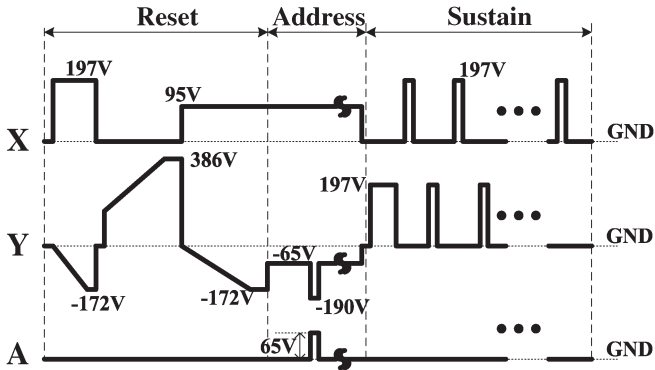| Front Panel		Rear Panel	
ITO width	225 μm	Barrier rib width	55 μm
ITO gap	85 μm	Barrier rib height	120 μm
Bus width	50 μm	Address width	95 μm
Pixel Pitch		912 μm × 693 μm	
Gas chemistry		Ne-Xe (11 %)-He (35 %)	
Barrier rib type		Closed rib	

Fig. 2. Schematic diagram of driving waveform used in this study.

and firing voltage, respectively. A 42-in panel with a working gas pressure of 400 torr was employed in this study, and its structure and dimensions were an XGA grade PDP with a box-type barrier rib. The gas mixtures used were Ne–He (35%)–Xe (11%). The detailed panel specifications are listed in Table I. The MgO thin film was deposited on the dielectric layer of the ac PDP by using ion-plating evaporation [15], and the oxygen and hydrogen flow rates were kept at 220 and 60 sccm, respectively, during the deposition.

To produce variously sputtered MgO states, the numbers of sustain discharge were controlled, so that the entire region of the 42-in panel was changed to a full-white background image immediately after displaying the square-type images (Cases 1–4) for about 1000 h.

Fig. 2 shows the conventional driving waveform with a selective reset waveform, including the reset, address, sustain periods employed in this study. The frequency for the sustain period was 200 kHz, the sustain voltage was 197 V, and the sustain pulsewidth was 2 μs. Table II shows the discharge conditions with different sustain numbers for producing vari-

TABLE II
COMPARISON OF DISCHARGE CONDITIONS WITH
DIFFERENT SUSTAIN PULSE NUMBERS

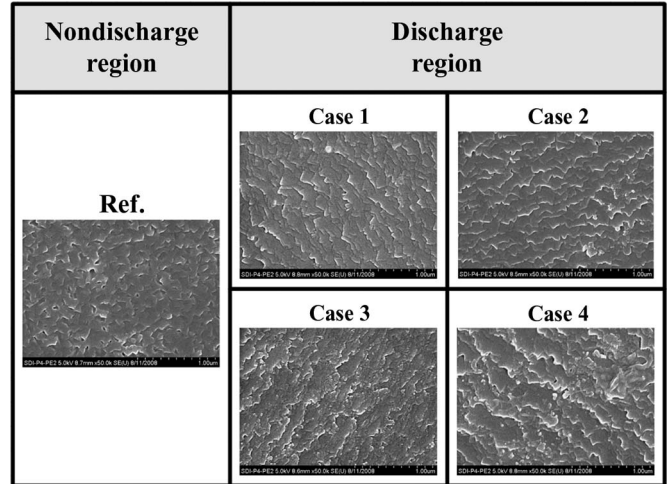|	Ref.	Case 1	Case 2	Case 3	Case 4
Sustain ON pulse number per 1-TV field	0	50	210	530	970
Discharge time [hr]	0	6	25.2	63.6	116.4

Fig. 3. Comparison of SEM images of MgO surface in nondischarge (Ref.) and discharge regions (Cases 1–4) relative to discharge time.

ously sputtered MgO states, where the reference case means the nondischarge case.

In the discharge region, where strong sustain discharges were repeatedly produced, Mg species were sputtered from the MgO surface due to the ion bombardment of the MgO protective layer during an iterant strong sustain discharge [16]; thus, Mg species were predominantly redeposited and deposited on the MgO and phosphor layers. To investigate the various sputtered MgO states, SEM, AFM, and SIMS were used to inspect the surface roughness, morphology, and impurity level of the MgO layer and analyze the Mg species deposited on the phosphor layer, respectively [16]. Furthermore, to investigate the changes in the electron emission characteristics of the MgO surface caused by the MgO surface changes, T_f and T_s were measured during the address period.

III. RESULTS AND DISCUSSION

A. Change in Surface Characteristics of MgO Layer Induced by Ion Bombardment

Fig. 3 shows the SEM images of the MgO surface for the nondischarge (Ref.) and discharge (Cases 1–4) regions. When comparing the nondischarge (Ref.) and discharge (Cases 1–4) regions, the pyramidal morphology of the grains on the MgO surface in the discharge region was found to have been eliminated, as shown by the SEM image in Fig. 3, which was mainly due to the ion bombardment during the sustain discharge. When increasing the number of sustain discharges, more grains were
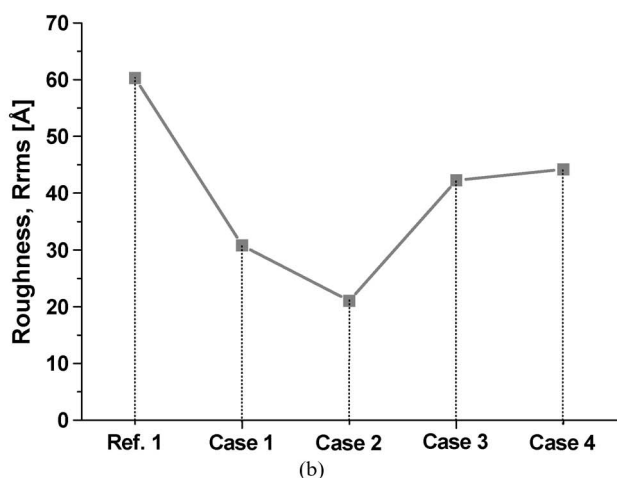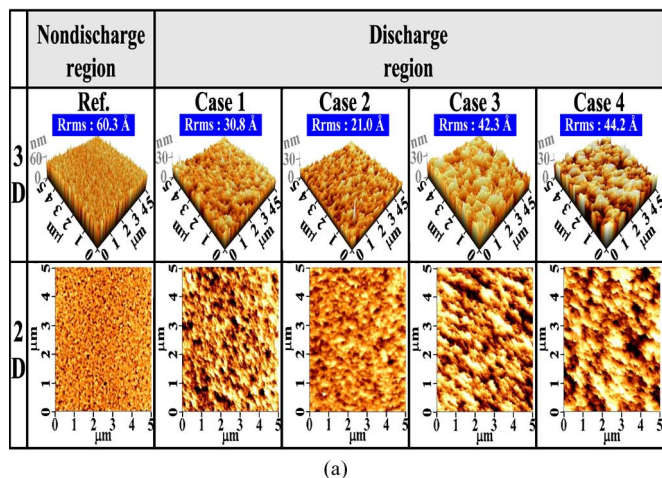
(a)

(b)

Fig. 4. Comparison of (a) 2- and 3-D AFM images of the MgO surface and (b) roughness of MgO surface based on AFM analysis in nondischarge (Ref.) and discharge regions (Cases 1–4) relative to discharge time.

removed from the MgO surface in the discharge region when compared with the nondischarge region, indicating that more Mg species, instead of oxygen particles, had been sputtered from the MgO layer.

Fig. 4(a) shows the 2-D and 3-D AFM images of the MgO surface for the nondischarge (Ref.) and discharge (Cases 1–4) regions. In particular, the 3-D AFM images in Fig. 4(a) indicated that the MgO surfaces were more damaged as the ion bombardment became severer. Fig. 4(b) shows the roughness of the MgO surface based on an AFM analysis for the nondischarge (Ref.) and discharge (Cases 1–4) regions. As shown in Fig. 4(a) and (b), compared with the nondischarge (Ref.) regions, the roughness of the MgO surface was lowest in Case 2. In Case 2, the roughness of the MgO surfaces in the discharge regions was smaller; this decreased roughness was mainly due to more on the sputtering of the MgO layer than on the redeposition of the MgO layer during the sustain discharge. In Case 3, the roughness of the MgO surfaces in the discharge regions was higher; this increased roughness was mainly due to the increase in the damage of the MgO layer, which was caused by repeated sputtering and redeposition on the MgO layer during the long-time sustain discharge.

The MgO layer was an ionic compound. This means that the ionic compound needs positive and negative ions to form the
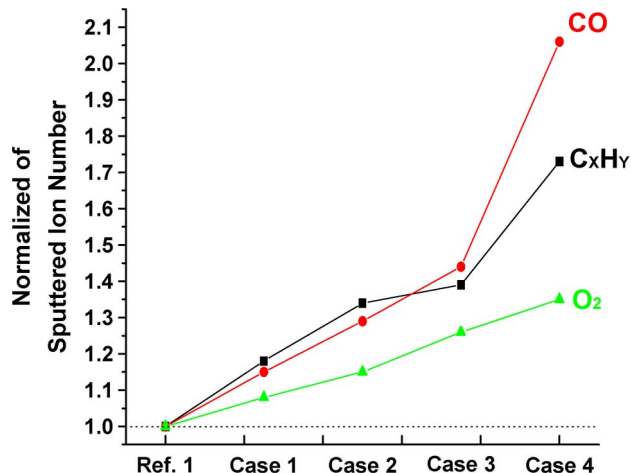

Fig. 5. Comparison of normalized SIMS data on MgO surface in nondischarge (Ref.) and discharge regions (Cases 1–4) relative to discharge time.

compound by columbic attraction. In the discharge region, Mg species were sputtered from the MgO surface due to the ion bombardment of the MgO protective layer during a repetitive strong sustain discharge. Thus, Mg species were predominantly redeposited and deposited on the MgO and phosphor layers, whereas the oxygen particles would be combined in the form of either CO or O_2. Fig. 5 shows the normalized impurity intensity on the MgO surface detected by a SIMS analysis relative to the discharge time. The SIMS in Fig. 5 measured the total count of the secondary ion emitted from the MgO surface, while the MgO surface was struck only for 100 s by the primary Bi ions from the ion gun with 25 keV. The primary ion beam energy was 1 pA, the measurement area was $150 \times 150 \ \mu m^2$, and the measurement depth was about 10 nm. The electron gun was not used to charge the dielectric MgO surface by the secondary ion when it was sputtered during measurement. As shown in Fig. 5, the impurities, such as CO, C_xH_y (organic), and O_2, increased with an increase in the ion bombardment. As such, the continuous production of plasma within the cells caused an outgas of impurities, such as C, H, and O, from the surfaces of the MgO, barrier rib, and phosphor layer, thereby increasing the impurities, such as CO, C_xH_y (organic), and O_2, as a result of activating a reaction on the MgO surface under ion bombardment during a repetitive strong sustain discharge.

B. Detection of Mg Particles on Phosphor Layer

Fig. 6(a) shows the Mg-depth profiles detected from the red phosphor layers for the nondischarge (Ref.) and discharge (Cases 1–4) regions using a SIMS analysis. Unlike the SIMS analysis on the MgO surface in Fig. 5, the Mg-depth profile in the SIMS analysis on the phosphor layer in Fig. 6(a) meant the amount of the Mg sputtered from the red phosphor layer while the O_2 ions struck the surface of the red phosphor layer for over 600 s. Fig. 6(b) shows the changes in the firing voltage for side V (Y–A) under a phosphor–cathode condition for the nondischarge (Ref.) and discharge (Cases 1–4) regions using V_t closed curve analysis [17]. When increasing the number of sustain discharges, the Mg ions detected from the red phosphor layer in the discharge region were increased when compared to that in the nondischarge region, indicating that more Mg species were
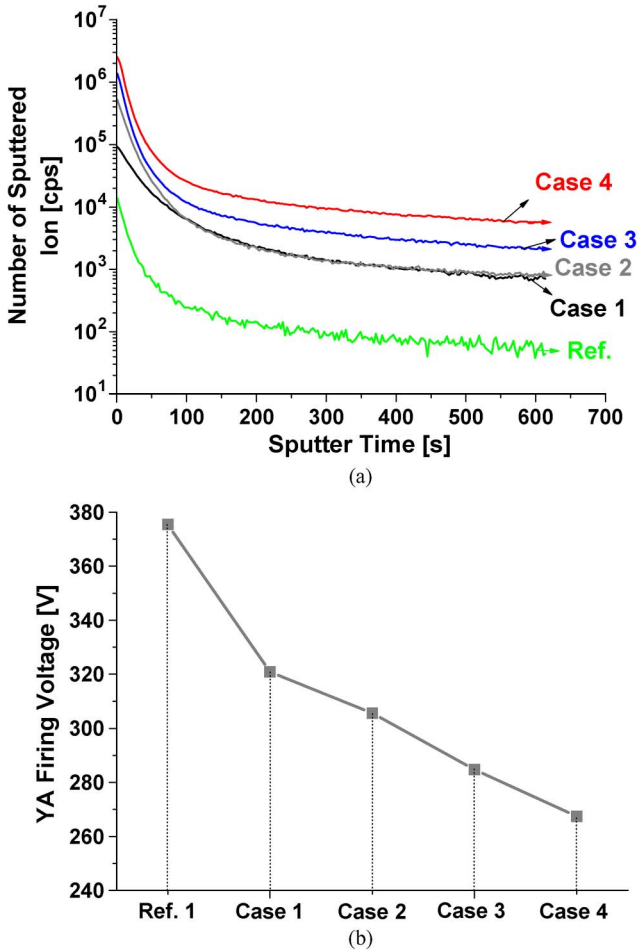
Fig. 6. Comparison of (a) Mg-depth profiles for red phosphor layer and (b) firing voltages between Y and A electrodes under phosphor–cathode condition in nondischarge (Ref.) and discharge regions (Cases 1–4) relative to discharge time. The firing voltages were measured using V_t closed curve method.

Fig. 7. Comparison of CL spectra for MgO layer in nondischarge (Ref.) and discharge regions (Cases 1–4) relative to discharge time.

deposited on the phosphor layer [16]. In Fig. 6(a), the sputtered secondary Mg ions were highest in Case 4, which showed that the largest amount of Mg was sputtered from the MgO layer in Case 4. The deposition of Mg species on the phosphor layer significantly affected the discharge characteristics, particularly under the phosphor–cathode condition. Therefore, as shown in Fig. 6(b), when increasing the number of sustain discharges, the firing voltage under the phosphor–cathode condition was decreased when compared to that in the nondischarge region. The reduction of the firing voltage in the Y–A plate gap discharges under the phosphor–cathode condition was presumably due to the deposit of a large amount of Mg species with a higher secondary electron emission coefficient on the phosphor layer, which was caused by the MgO sputtering induced by the iterant ion bombardment [16]. This result confirms that the increase in the number of sustain discharges would produce the severely sputtered MgO surface.

C. Change in CL Intensity of MgO Layer Induced by Ion Bombardment and Related Address Discharge Characteristics

The insulating materials, such as the magnesium oxide (MgO), also exhibited various types of defect (impurities, vacancies, etc.) that can play a significant role in the radiative
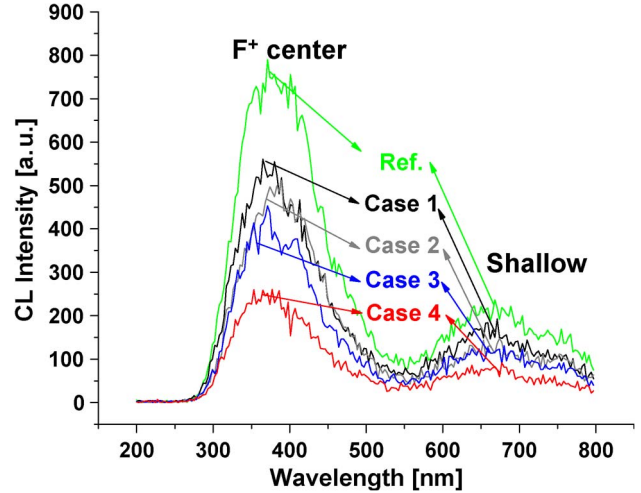
emission of the insulating materials. While free carriers (electrons or holes) interact and are captured by insulating materials, their detrapping is accompanied by phonon or radiative decay [6], [10].

The CL technique measures the defect levels of MgO film that can produce visible range radiation (1.8–3.5 eV). As the electron beam penetrates deep into the film, most of the signals are coming from the defects located deep inside the film. In the PDP cell, the sputtering or ion bombardment can also penetrate deep into the MgO thin film during a repetitive long-time sustain discharge [18]. Therefore, to investigate the changes in the defect levels of the MgO layer due to the ion bombardment, the radiative emissions of various sputtered MgO states are examined by using the CL technique.

Fig. 7 shows the changes in the CL intensity of the MgO layer in the nondischarge (Ref.) and discharge (Cases 1-4) regions for various sputtered MgO states. For the two peaks showing the CL intensity in Fig. 7, the F^+ center peak (387.5 nm) with a level of 3.2 eV was related to the secondary electron emission, whereas the shallow peak (670.2 nm) with a level of 1.85 eV was related to the electron emission from the shallow level. When increasing the ion bombardment, the F^+ center peak of the CL intensity decreased, indicating that the electron emission capability of the MgO layer was reduced as a result of severe ion bombardment. Moreover, when increasing the ion bombardment, the shallow level peak of the CL intensity was decreased, implying that the electron emission capability from the shallow level of the MgO layer was also reduced as a result of severe ion bombardment. Thus, the effect of the variations in the electron emission characteristics of the MgO layer induced by severe ion bombardment on the address discharge during the address period was analyzed by monitoring the changes in T_f, T_s, and ΔV_w.

Fig. 8 shows the changes in T_f and T_s relative to the discharge time. Fig. 8 also shows the changes in ΔV_w between the A and Y electrodes based on the V_t closed curves relative to the discharge time [7], [19]. ΔV_w meant the difference of the wall voltages from the first to the last scan line between the A and Y electrodes. As shown in Fig. 8, severe ion bombardment
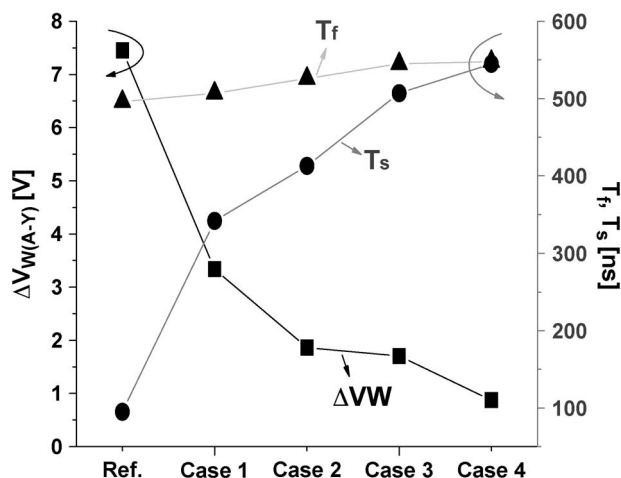
Fig. 8. Variation in T_f, T_s, and ΔV_w for nondischarge (Ref.) and discharge regions (Cases 1–4) relative to discharge time.

caused an increase in T_f when compared to the nondischarge region. Severe ion bombardment induced predominant sputtering of Mg species from the MgO surface, which was verified by the decrease in the F^+ center peak in the CL intensity, thereby reducing the defect levels in the MgO layer and leading to an increase in T_f [20], [21]. Meanwhile, as shown in Fig. 8, severe ion bombardment also caused an increase in T_s, yet a decrease in ΔV_w, when compared with the nondischarge region. Severe ion bombardment caused a decrease in the intensity of the shallow level of the MgO layer, thereby reducing the electron emissions from shallow levels that act as priming particles in the discharge space. Accordingly, it is suggested that a 670.2-nm emission peak from the shallow level might be a possible indicator of exoelectron emission characteristics from the MgO layer [9], [11], [12]. As a result, T_s was increased, while ΔV_w was reduced, due to poor exoelectron emission characteristics [7]–[9], [14]. As severe ion bombardment destroys the trap levels in the MgO layer, the intensity of the shallow level was decreased, as shown by the CL peak in Fig. 7. However, as shown by the SIMS data in Fig. 5, the increase in H, C, or O on the MgO surface due to the ion bombardment did not help in constituting the trap levels of the MgO layer, which was simply due to the sputter or redeposit of MgO resulting from the severe ion bombardment.

IV. CONCLUSION

The address discharge characteristics and CL intensity have been found to be strongly related to the MgO surface sputtered by an iterant strong ion bombardment. Severe ion bombardment during a sustain discharge induced predominant sputtering of Mg species from the MgO surface, thereby lowering the intensity of the F^+ center peak due to the elimination of the oxygen vacancy and eventually leading to an increase in T_f. Meanwhile, severe ion bombardment during a sustain discharge also destroyed the shallow trap level, thereby lowering the intensity of the shallow peak and eventually leading to an increase in T_s and reduction of ΔV_w.

REFERENCES

[1] L. F. Weber, "In celebration of 40 years of PDP history," in *Proc. IDW Dig.*, 2004, pp. 859–862.
[2] D.-K. Lee, C.-H. Park, H. J. Lee, W.-S. Choi, D.-H. Kim, and H.-J. Lee, "Electro-optical characteristics of plasma display panel with $Mg_{1-x}Si_xO$ protecting thin films deposited by an electron-beam evaporation method," *Appl. Phys. Lett.*, vol. 89, no. 19, pp. 191501-1–191501-3, Nov. 2006.
[3] S.-H. Yoon, C.-R. Hong, J. J. Ko, H.-S. Yang, and Y.-S. Kim, "Measurement of exo-electron emission from MgO thin film of ACPDPs," *J. Soc. Inf. Displ.*, vol. 17, no. 2, pp. 131–136, Feb. 2009.
[4] T. Okada and T. Yoshioka, "Application of carbon nanotubes as a source of priming electrons in ac plasma display panels," *Appl. Phys. Lett.*, vol. 93, no. 17, pp. 171501-1–171501-3, Oct. 2008.
[5] T. Okada, T. Naoi, and T. Yoshioka, "Decay kinetics of luminescence and electron emission from MgO crystal powders in ac plasma display panel," *J. Appl. Phys.*, vol. 105, no. 11, pp. 113304-1–113304-10, Jun. 2009.
[6] M. Ghamnia, C. Jardin, and M. Bouslama, "Luminescent centres F and F^+ in α-alumina detected by cathodoluminescence technique," *J. Electron Spectrosc. Relat. Phenom.*, vol. 133, no. 1–3, pp. 55–63, Nov. 2003.
[7] T. Okada, T. Furutani, and T. Yoshioka, "Decay kinetics of electron emission from MgO films in AC plasma display panel," *Appl. Phys. Express*, vol. 1, no. 9, pp. 091203-1–091203-3, Sep. 2008.
[8] Q. Yan, N. Kosugi, Y. Oe, H. Tachibana, and L. F. Weber, "Analysis of priming source for addressing discharge of AC PDP," in *Proc. IDW Dig.*, 2006, pp. 359–362.
[9] H. Tolner, "Exo-electron emission effects in the PDP protective layer," in *Proc. ASID Dig.*, 2006, pp. 136–143.
[10] Y. Motoyama, Y. Hirano, K. Ishii, Y. Murakami, and F. Sato, "Influence of defect states on the secondary electron emission yield γ from MgO surface," *J. Appl. Phys.*, vol. 95, no. 2, pp. 8419–8424, Jun. 2004.
[11] G. H. Rosenblatt, M. W. Rowe, G. P. Williams, Jr., and R. T. Williams, "Luminescence of F and F^+ centers in magnesium oxide," *Phys. Rev. B, Condens. Matter*, vol. 39, no. 14, pp. 10 309–10 318, May 1989.
[12] H. Tolner, "The physics and processing of exo-emission in MgO," in *Proc. IDW Dig.*, 2006, pp. 333–336.
[13] T. Hirakawa and H. Uchiike, "A study of evaporated MgO thin film by cathodoluminescence," in *Proc. IDW Dig.*, 2003, pp. 873–876.
[14] K.-H. Park and Y.-S. Kim, "Characteristics of MgO layer deposited under hydrogen atmosphere," in *Proc. SID Dig.*, 2006, pp. 1395–1398.
[15] G. S. Lee, K. B. Kim, J. J. Kim, and S. H. Sohn, "Effects of hydrogen doping on surface and discharge properties of MgO thin films grown by ion plating," *J. Phys. D, Appl. Phys.*, vol. 42, no. 10, pp. 105 402-1–105 402-5, Apr. 2009.
[16] C.-S. Park, H.-S. Tae, Y.-K. Kwon, and E. G. Heo, "Experimental observation of halo-type boundary image sticking in AC plasma display panel," *IEEE Trans. Electron Devices*, vol. 54, no. 6, pp. 1315–1320, Jun. 2007.
[17] K. Sakita, K. Takayama, K. Awamoto, and Y. Hashimoto, "High-speed address driving waveform analysis using wall voltage transfer function for three terminal and Vt close curve in three-electrode surface-discharge AC-PDPs," in *Proc. SID Dig.*, 2001, pp. 1022–1025.
[18] C.-S. Park and H.-S. Tae, "Solutions to remove a boundary image sticking in an ac plasma display panel," *Appl. Opt.*, vol. 48, no. 25, pp. F76–F81, Sep. 2009.
[19] S.-K. Jang, H.-S. Tae, E.-Y. Jung, J.-C. Ahn, J.-H. Oh, and E. G. Heo, "Driving waveform with multi-scan high level for stable address discharge under variable ambient temperature," in *Proc. SID Dig.*, 2008, pp. 1729–1732.
[20] Y. Cho, C. Kim, H.-S. Ahn, E. Cho, T.-E. Kim, and S. Han, "First-principles study on secondary electron emission of MgO surface," *J. Appl. Phys.*, vol. 101, no. 8, pp. 083710-1–083710-7, Apr. 2007.
[21] H.-S. Ahn, T.-E. Kim, E. Cho, M. Ji, C.-K. Lee, S. Han, Y. Cho, and C. Kim, "Molecular dynamics study on low-energy sputtering properties of MgO surface," *J. Appl. Phys.*, vol. 103, no. 7, pp. 073518-1–073518-9, Apr. 2008.

Choon-Sang Park received the M.S. and Ph.D. degrees in electronic and electrical engineering from Kyungpook National University, Daegu, Korea, in 2006 and 2010, respectively.

Since 2010, he has been a Postdoctoral Fellow with the School of Electrical Engineering and Computer Science, Kyungpook National University. His current research interests include microdischarge physics, MgO thin film, driving waveform of plasma display panels, and surface analysis for new materials.

Heung-Sik Tae (M'00–SM'05) received the B.S., M.S., and Ph.D. degrees in electrical engineering from Seoul National University, Seoul, Korea, in 1986, 1988, and 1994, respectively.

Since 1995, he has been a Professor with the School of Electrical Engineering and Computer Science, Kyungpook National University, Daegu, Korea. His research interests include the optical characterization and driving waveform of plasma display panels, the design of millimeter-wave guiding structures, and electromagnetic wave propagation using meta-materials.

Dr. Tae is a member of the Society for Information Display. He has been serving as an Editor for the IEEE TRANSACTIONS ON ELECTRON DEVICES section on display technology since 2005.

Eun-Young Jung received the B.S. degree in physics from Daegu Catholic University, Kyungpook, Korea, in 1998 and the M.S. and Ph.D. degrees in physics from Kyungpook National University, Daegu, Korea, in 2000 and 2006, respectively.

From 2000 to 2003, she was an Assistant Manager of the PDP division, Orion PDP Company Ltd., Kyungpook. From 2003 to 2009, she was also an Assistant Manager of the PDP division, Samsung SDI Company Ltd., Cheonan, Korea. Since 2009, she has been a Senior Manager of the Core Technology Laboratory, Corporate R&D Center, Samsung SDI Company Ltd., Cheonan, Korea. Her current research interests include MgO thin film, simulation analysis, microdischarge physics for plasma display panels, and surface analysis for new materials.

Jeong Hyun Seo received the B.S. degree in electrical engineering and the M.S. and Ph.D. degrees in plasma engineering from Seoul National University, Seoul, Korea, in 1993, 1995, and 2000, respectively.

From 2000 to 2002, he was with the plasma display panel (PDP) division, Samsung SDI, Cheonan, Korea, where his work focused on the design of driving pulse in ac PDP. Since September 1, 2002, he has been a Professor with the Department of Electronics Engineering, University of Incheon, Incheon, Korea. His research is currently focused on the high-efficiency PDP cell structure, driving method, and numerical modeling in PDP.

Dr. Seo is a member of the Society for Information Display and the Korean Information Display Society.

Bhum Jae Shin received the B.S. degree in electrical engineering and the M.S. and Ph.D. degrees in plasma engineering from Seoul National University, Seoul, Korea, in 1990, 1992, and 1997, respectively.

From 1997 to 2000, he was a Senior Researcher with the PDP team, Samsung SDI, Korea, working on the development of PDPs. From 2000 to 2001, he was a Visiting Researcher with the Physics Department, Stevens Institute of Technology, Hoboken, NJ, working on capillary discharges. In 2002, he returned to Korea, and following a one-year Postdoctoral at Seoul National University, he is currently a Research Professor with the Department of Electronics Engineering, Sejong University, Seoul. His research interests include high-efficiency PDP cell structure and driving scheme.

Dr. Shin is a member of the Society for Information Display and the Korean Information Display Society.